Developmental Biology 371 (2012) 94–109

Contents lists available at SciVerse ScienceDirect

Developmental Biology

journal homepage: www.elsevier.com/locate/developmentalbiology

Evolution of Developmental Control Mechanisms

Independent migration of cell populations in the early gastrulation of the amphipod crustacean *Parhyale hawaiensis*

R. Crystal Chaw [a,*,1], Nipam H. Patel [b]

[a] Department of Integrative Biology, University of California Berkeley, Berkeley, CA 94720-3200, USA
[b] Departments of Integrative Biology and Molecular and Cell Biology, University of California Berkeley, Berkeley, CA 94720-3200, USA

ARTICLE INFO

Article history:
Received 26 June 2012
Received in revised form
15 August 2012
Accepted 19 August 2012
Available online 27 August 2012

Keywords:
Gastrulation
Arthropod
Crustacean Morphogenesis
Cell-shape change
Embryogenesis

ABSTRACT

Cells are the principal component of tissues and can drive morphogenesis through dynamic changes in structure and interaction. During gastrulation, the primary morphogenetic event of early development, cells change shape, exchange neighbors, and migrate long distances to establish cell layers that will form the tissues of the adult animal. Outside of *Drosophila,* little is known about how changes in cell behavior might drive gastrulation among arthropods. Here, we focus on three cell populations that form two aggregations during early gastrulation in the crustacean *Parhyale hawaiensis.* Using cytoskeletal markers and lineage tracing we observe bottle cells in anterior and visceral mesoderm precursors as gastrulation commences, and find that both Cytochalasin D, an inhibitor of actin polymerization, and ROCKOUT, an inhibitor of Rho-kinase activity, prevent gastrulation. Furthermore, by ablating specific cells, we show that each of the three populations acts independently during gastrulation, confirming previous hypotheses that cell behavior during *Parhyale* gastrulation relies on intrinsic signals instead of an inductive mechanism.

Introduction

How does morphogenesis occur? Among arthropods, research with the fruit fly *Drosophila melanogaster* has provided important clues about the molecular mechanisms regulating embryonic patterning and morphogenesis. Comparison with additional arthropod species contributes to our understanding of the evolution of early patterning, but relatively few comparative investigations focus on the cellular dynamics that drive morphogenesis. Gastrulation, which is a crucial morphogenetic event during early embryonic development among metazoans, has a long history of studies focused on cellular behavior, mechanics, and interaction (for review see Stern (2004)). During gastrulation, cells undergo dynamic changes toward the establishment of the embryonic germ layers that will give rise to the various systems of the adult. Cell behavior during gastrulation is an important and experimentally tractable manifestation of the molecular patterning that results in the morphology of an animal. Because cellular gastrulation strategies can vary widely from species to species, meaningful evolutionary comparisons can only be made through sampling a wide variety of taxa (Stern, 2004; Davidson, 2008).

Outside of *Drosophila*, little is known about how changes in cell behavior or cellular interactions drive gastrulation in arthropods. In the emerging model crustacean *Parhyale hawaiensis* (Amphipoda), gastrulation is multi-phasic and begins with the formation of two spatially and visually distinct cell populations, the rosette and the epithelial sheet (Gerberding et al., 2002; Browne et al., 2005; Price and Patel, 2008; Alwes et al., 2011; see Fig. 1). The rosette, which is comprised of germline and anterior and visceral mesoderm precursors, gastrulates underneath the ectodermal precursors of the epithelial sheet to form a multilayered germ disc that is a condensation of cells that will form the embryo proper. The somatic mesoderm and endoderm internalize later (Gerberding et al., 2002; Browne et al., 2005; Price and Patel, 2008; Alwes et al., 2011; see Fig. 1 and the following paragraph). Multiple phases of gastrulation are not unique to *Parhyale*. Most insects have temporally distinct internalization of mesoderm and endoderm (Roth, 2004), and there are examples among crustaceans and chelicerates where mesendoderm is internalized at different times (Gerberding and Patel 2004; Anderson, 1973). For example, the germline and mesendoderm precursors of another amphipod crustacean, *Orchestia cavimana*, form a cluster that is outlined by a sickle-shaped collection of ectoderm precursors. The presumptive germline initiates gastrulation by sinking into the yolk. A later phase of *Orchestia* gastrulation involves internalization of the mesendoderm and somatic mesoderm (Wolff and Scholtz, 2002; Scholtz and Wolff, 2002). Among chelicerates, canonical spider development features the internalization of

* Corresponding author. Fax: +1 951 827 4286.
E-mail addresses: rocrystalchaw@gmail.com, rcrystal@ucr.edu (R.C. Chaw).
[1] Present address: Department of Biology, University of California Riverside, Riverside, CA 92521, USA.

0012-1606/$ - see front matter © 2012 Elsevier Inc. All rights reserved.
http://dx.doi.org/10.1016/j.ydbio.2012.08.012

mesendodermal cells that form the "primitive plate"(Anderson, 1973; Foelix, 1996). The primitive plate includes a smaller collection of mesenchymal cells, called the "cumulus," that break away from the main group of cells and migrate underneath the nascent germ disc. The continued internalization of mesendoderm occurs during and after cumulus migration.

Because of an 8-cell fate map and extensive lineage tracing, the cellular origin and composition of the *Parhyale* rosette and epithelial sheet are well understood (Gerberding et al., 2002; Alwes et al., 2011). The first three *Parhyale* cleavages are total. The third cleavage is highly unequal and results in an 8-cell embryo with four micromeres and four macromeres. Based on the position of the polar bodies, the animal hemisphere is associated with the yolkier macromeres while the vegetal hemisphere is associated with the less yolky micromeres. The embryo then transitions to asynchronous and asymmetrical cleavages that result in repositioning the yolk to the center of the embryo. Cells after this stage are at the periphery of the egg and are of approximately the same size due to accelerated cleavage of the macromeres (Browne et al., 2005; Alwes et al., 2011). At this point, approximately 12 h post-fertilization (hpf) at 26 °C, the rosette and the epithelial sheet begin to form. The rosette is a cluster of roughly 12–16 cells comprising descendants from the sister 8-cell blastomeres **Mav** and **g**, and the epithelial sheet is a cluster of roughly 50 cells made of descendants from the blastomeres **El, Er,** and **Ep** (Gerberding et al., 2002; Browne et al., 2005; Alwes et al., 2011; See Figs. 1 and 2). The rosette and the epithelial sheet develop on opposing sides of the egg, with the rosette developing on the vegetal half and marking the future anterior end of the embryo (Browne et al., 2005). Prior to formation of the germ disc, the rosette and epithelial sheet are easily distinguished with brightfield microscopy and/or lineage tracing. After germ disc formation, the two populations are discernible in vivo using lineage tracing with fluorescent dyes and/or mRNA constructs (Gerberding et al., 2002). Descendants of the blastomeres **ml, mr,** and **en** give rise to the left, right somatic mesoderm and endoderm, respectively. These precursors ingress and remain under the surface after germ disc condensation has already begun (Gerberding et al., 2002; Browne et al., 2005; Alwes et al., 2011; Fig. 1).

Lineage tracing has led to current hypotheses that the *Parhyale* rosette internalizes through ingression or invagination combined with epiboly of the epithelial sheet (Gerberding et al., 2002; Browne et al., 2005; Price and Patel, 2008). While similar descriptive studies implicate ingression and invagination as mechanisms for cell internalization in additional crustacean species, there are, however, also species that primarily gastrulate through delamination or oriented cell division (Gerberding and Patel, 2004). Treatment of *Parhyale* embryos with an inhibitor of zygotic transcription did not prevent rosette internalization, but did affect normal germ disc formation. This suggests that the inward migration of rosette cells proceeds independently of the epithelial sheet, but that normal epiboly of ectoderm precursors relies on zygotic transcription-dependent signaling through cell–cell contact with the rosette (Alwes et al., 2011). Reliance on cell-to-cell contact during gastrulation would be consistent with some other crustaceans and chelicerates. Hertzler et al. (1994) cultured blastomeres isolated from 2-, 4-, 8-, and 16-cell *Sicyonia ingentis* (shrimp) embryos and found that the mesendodermal D blastomere undergoes gastrulation regardless of its cell–cell contacts provided there are enough cells to form an archenteron. Without the D blastomere, the other blastomeres never progress beyond blastulae. Not only does this indicate that cell fates are determined early, but also suggests that the D blastomere may induce neighboring cells to form portions of the archenteron (Hertzler et al., 1994). Interestingly, cells in the cumulus of the spider *Parasteatoda tepidariorium* have been shown to signal with the

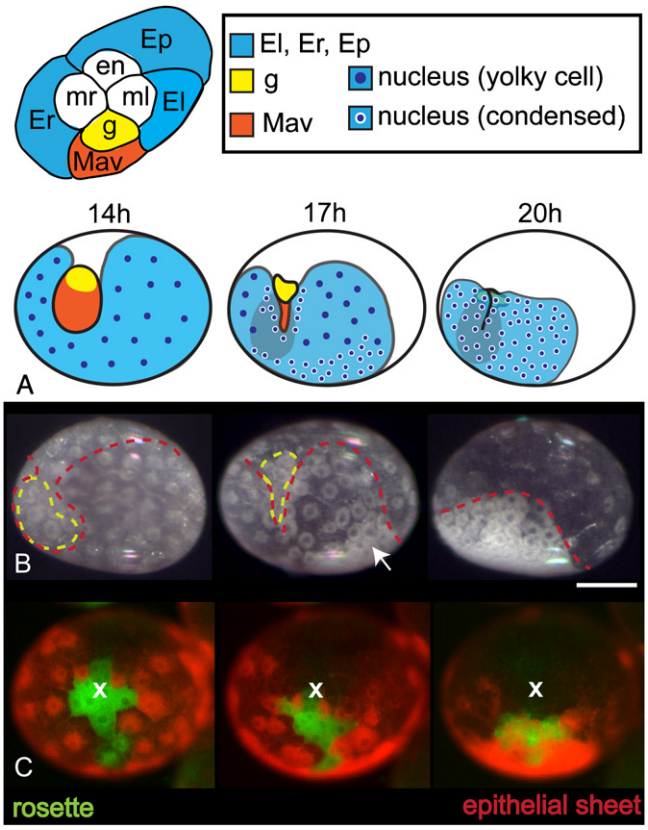

Fig. 1. Two embryos and a schematic show a vegetal view of the first phase of gastrulation. (A) The *Parhyale* fate map at the 8-cell stage (top) and a schematic of the rosette and the epithelial sheet during rosette internalization (bottom). Blastomeres that give rise to the rosette are the anterior and visceral mesoderm (Mav, orange) and the germline (g, yellow). Blastomeres that give rise to the epithelial sheet are the left, right, and posterior ectoderm (El, Er, and Ep, respectively; blue). Colors correspond to Price and Patel (2008). The left and right somatic mesoderm (ml and mr) and the endoderm (en) are not colored and are left in white. (B) Brightfield images of a single embryo at 14 hpf, 17 hpf, and 20 hpf of development at 26 °C. Dashed lines estimate areas covered by the rosette (yellow) and the epithelial sheet (red). Area outside the dashed line corresponds to white area in (A). Arrow at 17 hpf indicates condensing and migrating epithelial sheet cells, some of these cells originated on the animal half of the embryo. By 20 hpf, the rosette is no longer visible underneath the condensed epithelial sheet cells. (C) The rosette and epithelial sheet move to one side of the embryo during internalization. Stills were taken from a timelapse video of embryos embedded in agarose and filmed at room temperature (~22 °C). Images are cropped to focus on a single embryo. Blastomeres were microinjected at the 8-cell stage to label the rosette (FITC, green) and the epithelial sheet (TRITC, red). Stills were chosen to match staging of brightfield images; total elapsed time from left to right image is 8 h. Although some natural variability in egg shape does occur, the rosette looks different than in B because the embryo is rotated slightly and pressed against the glass to centralize and focus on the rosette. Dark unlabeled area corresponds to the white area in (A) and the area outside the dashed lines in (B). X indicates the approximate center of the rosette before internalization. Scale bar is 100 μm.

morphogen *decapentaplegic* to overlying ectoderm precursors (Akiyama-Oda and Oda, 2003; *Parasteatoda* was reclassified from *Achaearanea* by Saaristo (2006)). This signal is thought to help define the dorso-ventral and anterior–posterior axes of the developing embryo (Akiyama-Oda and Oda, 2006). Furthermore, removal of the cumulus in the spider *Agelena labrynthica* results in radialized embryos, and transplantation of cumulus cells to a different area of the germ disc induces twinning (Holm, 1952).

In this study, we investigate cell-shape change in the cell types that comprise the *Parhyale* rosette, treat gastrulating embryos with pharmacological inhibitors of the actin cytoskeleton and the actin regulator Rho-kinase, and ablate portions of the rosette and the epithelial sheet immediately prior to and during gastrulation. Cell-shape changes and the actin cytoskeleton are key components of cell

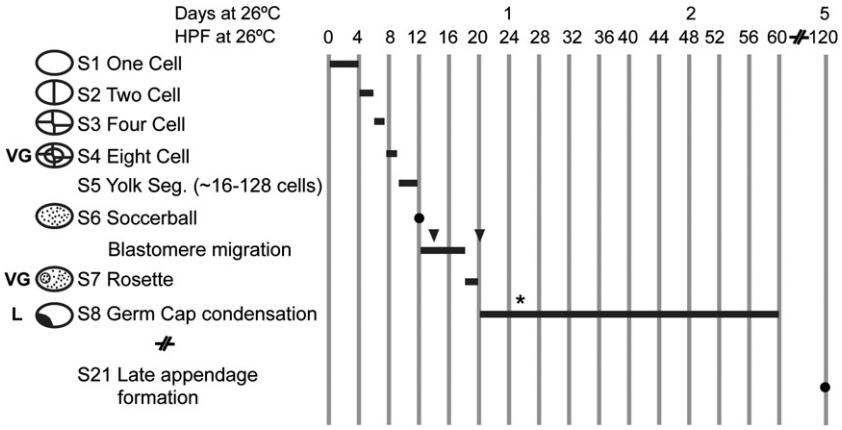

Fig. 2. Diagram of relevant stages of *Parhyale* embryogenesis. Axis corresponding to days of development and hours post-fertilization (HPF) runs from left to right across the top. Stage schematic, stage number, and a short description run from top to bottom at the left. Arrowheads indicate beginning of rosette formation (approximately 13 hpf) and end of rosette internalization (approximately 20 hpf). Asterisk indicates the end of gastrulation (germ disc stage, S8, 25 hpf). VG=vegetal view, *L*=lateral view. After Browne et al. (2005).

behavior. When gastrulating, cells undergo characteristic changes in morphology such as apical constriction. The active narrowing of cellular apices is associated with ingression, invagination, and epithelial to mesenchymal transitions in examples of morphogenesis and cell migration across taxa (Sawyer et al., 2010). Changes in cell morphology that are associated with apical constriction include shifting of the nucleus toward the basal end of the cell, the concentration of actin to the apical side of the cell, and the formation of "bottle cells," which are cells with a narrow apex and broad base (Holtfreter, 1943; Hardin and Keller, 1988). Bottle cells were first observed during gastrulation in the frog *Xenopus laevis* (Holtfreter, 1943). They have since been discovered during morphogenesis in a wide variety of taxa, are known to contribute to tissue remodeling, and are associated with ingression, invagination, and epithelial-to-mesenchymal transitions (Holtfreter, 1943; Hardin and Keller, 1988; Sawyer et al., 2010).

Cell behavior and cellular interactions during gastrulation are often studied through pharmacological treatments and cell ablation. The actin cytoskeleton, acto-myosin contractility, and regulators of cell polarity are popular targets for pharmacological manipulation because actin is the cytoskeletal component that is most often implicated in migration and cell-shape change (Jacinto and Baum, 2003; Ridley et al., 2003). Actin and myosin coordinate to form a contractile network that enables cell-shape changes such as apical constriction. One function of the *Rho* family of small GTPases is to regulate acto-myosin contractility by directly phosphorylating myosin (Jaffe and Hall, 2005). Phosphorylated myosin slides actin filaments over each other to shorten their overall length, causing the contraction that occurs during apical constriction (Sawyer et al., 2010). For example, gastrulation in the fruit fly *Drosophila* begins when a sub-population of ventral mesoderm precursors apically constricts. In these cells, RhoGEF2 works with the heteromeric g-protein Concertina to activate the downstream target *rho-kinase* (*ROCK*), which then phosphorylates myosin in the apical domain of cells (Nikolaidou and Barrett, 2004; Dawes-Hoang et al., 2005; Kölsch et al., 2007). In other systems, the Rho-ROCK pathway has been implicated in a variety of cytoskeletal processes, including regulating assembly of the actin cytoskeleton and thereby regulating cell polarity (Riento and Ridley, 2003).

Cell ablation investigates whether cells are acting independently or whether they rely on cell–cell communication. The above example in *S. ingentis* shows how removing cells can reveal an inductive mechanism. Conversely, in the nematode *Caenorhabditis elegans*, culturing pre-gastrula blastomeres in isolation and in various cell pairings revealed that each cell is capable of going through gastrulation movements without specific cell–cell contacts (Lee and Goldstein, 2003).

Although previous work investigates the gastrulation effects of ablating individual blastomeres early in development (Alwes et al., 2011), this study directly manipulates cells in the rosette and the epithelial sheet during gastrulation to investigate the cellular behavior and interactions that drive rosette internalization.

Materials and methods

Husbandry, dissection, and fixation

Embryos were staged according to Browne et al. (2005). Throughout the results section, we refer to the following stages: 4-cell (S3, ~7 hpf at 26 °C); 8-cell (S4, ~8 hpf); soccerball (S6, ~12 hpf); rosette (S7, ~18 hpf); germ disc (S8, ~25 hpf); and late appendage formation (S21, ~120 hpf) (See Fig. 2 for reference). We ablated and labeled lineages at the 4- and 8-cell stages. The rosette and epithelial sheet begin formation shortly after soccerball, rosette internalization occurs from approximately 17 hpf through 20 hpf, and gastrulation finishes by the germ disc stage (25 hpf), and we used late appendage stages to check for normal migration of the germline.

Husbandry and embryo collection, fixation, and dissection were done according to Rehm et al. (2009a) with minor changes. Pre-germ band embryos were placed in hypersaline fix (80% artificial seawater (ASW), 10% 10× Phosphate-buffered Saline (PBS), 3.7% formaldehyde) for 1 min and then transferred to seawater fix (3.7% formaldehyde in ASW). This causes tissue/chorion separation, facilitating dissection. All fixed embryos were rinsed (three quick washes) with ASW and then stored at 4 °C or washed into PT (0.1% Triton-X 100 in PBS) for immediate sectioning or antibody staining.

Thick sectioning

Fixed embryos were embedded in plastic molds with 2.5% low melt agarose (Promega V211) in PBS. The agarose mixture was heated to boiling and then cooled to 37° C. Embryos were embedded and oriented using forceps and a hypodermic needle. Each block was sectioned into a PBS bath using a Pelco 101

vibratome (speed 5.5, amplitude 4.5). Sections were approximately 80 μm thick.

Antibody and phalloidin staining of whole embryos and sections

Antibody staining was performed according to Rehm et al. (2009b) except that phalloidin was sometimes added to the secondary antibody incubation. We used the following (with concentrations): Rabbit anti-zebrafish Vasa (Gift from Nüsslein-Volhard lab, 1:1000; Knaut et al., 2000), Rat anti-Tubulin (Abcam; 1:500), Rabbit anti-dsRed (Clontech, 1:250), Alexa fluor goat anti-rat 488 and 647; goat anti-rabbit 546 and 555 (Molecular Probes; 1:1000), phalloidin 488 (Invitrogen, 1:40 of 6.6 μM stock). Vasa is a highly conserved transcriptional repressor restricted to the germline throughout metazoa and cross-reactive antibodies identify the germline in *Parhyale* (Extavour, 2005; Ozhan-Kizil et al., 2009).

Timelapse video

Embryos were filmed in ASW, drug solution, or embedded in a drop of 1.5% low melt agarose in ASW in glass-bottom dishes (Mattek, P35G-1.0-14-C). Dishes with embryos in agarose drops were filled with 70% ASW to prevent desiccation. Capture was at 5× or 10× in 5 min intervals on inverted scopes (Zeiss Axiovert 200 m or an AxioObserver.z1 using a Hammamatsu Orca-ER or Orca-R2 camera, respectively) using PerkinElmer's Volocity Acquisition software (v. 5.5.1 or v. 5.4.1).

Microinjection

Microinjection was done as previously described (Rehm et al., 2009c; Price et al., 2010). We injected the following (with concentrations): FITC (Fluorescein isothiocyanate–dextran, Sigma FD250S, 2 mg/ml or 5 mg/ml); TRITC (Tetramethylrhodamine isothiocyanate–dextran, Sigma T1287, 2 mg/ml); and/or an mRNA encoding a nuclear-localized dsRed protein (dsRed-NLS; 1ug/mL; Gerberding et al., 2002) (See Table 2 for a summary of injections). Two mg/mL of FITC is adequate for visualization but not photoablation. Embryos were kept at 26 °C or 18 °C. We injected approximately 15 or 110 picoliters into micromeres or macromeres, respectively. For all timelapse and ablation experiments, only embryos that where healthy after injection and that followed the majority cell division pattern, as described by Alwes et al. (2011), were used (Gerberding et al., 2002; Alwes et al., 2011). We did not observe any unusual deviations from division patterns that were previously reported (Gerberding et al., 2002; Alwes et al., 2011).

Photoablation

We modified previous photoablation protocols (Price et al., 2010). Broods of embryos develop near synchronously. A single brood of embryos was injected, allowed to develop and then half were subject to photoablation and the other half were used as controls.

Ablation proceeded in one of two ways: First, all embryos were agarose embedded with FITC injected cells against the glass in glass-bottom dishes. Then, embryos were either exposed to 100% mercury lamp power at 10× or 5× on an inverted scope using Zeiss filter set 17 (excitation: BP 485/20) for 30 min; or, specific cells were photoablated on a Zeiss 700 confocal using "regions" and "photobleaching" commands (Figs. 12, 13 and 14). The user-specified region fell within cell boundaries. Scanning proceeded at 100% laser power for 15 min at 10× on, at most, two embryos from each brood.

We used photobleaching as an immediate ablation marker (Price et al., 2010), and confirmed that these cells cease division and eventually lyse. Dead cytoplasm is exuded or reabsorbed. In all cases, the behavior of the remaining blastomeres was the same.

For filming, ablated embryos were agarose embedded with control embryos.

Manual ablation

At the 8-cell stage, we injected ~520 picoliters of a mixture of DNAse (10 units; Roche, #04716728001), two kinds of RNAse (RNAseA.01 mg, Sigma # R-5000; RNAse T1 10 units, Sigma R-1003), and TRITC (as a marker; 10 mg/ml) into the cell we wanted to ablate and then incubated the embryos at 31 °C for 2 h. In all cases, the injected blastomere ceased division and lysed. Capillary action from a pulled glass needle broken to a wide bore (~0.024 mm) completely removed cell debris through the injection site or through additional holes made with forceps. Embryos were then kept at 26 °C.

Cell tracing and analysis

Manual cell tracing was done over 157 frames with Volocity (PerkinElmer, v. 5.4, "Track Objects Manually"), from approximately 12 hpf (soccerball stage, S6) through 25 hpf (germ disc, S8). Tracing was limited to embryos that survived for at least 24 h.

We traced three epithelial sheet cells in each embryo ($n=14$ ablated, $n=12$ control embryos, Figs. 9 and 10): a "near" cell adjacent to the rosette on the side toward which post-internalization rosette and epithelial sheet migration would occur; a "far" cell on the opposite side of the rosette, away from the direction of migration; and a third "farthest" cell that was at least one-cell width away from the rosette on the far side (Figs. 9 and 10). From our observations and those of Alwes et al., (2011), all traced cells were El or Er progeny. When a cell cleaved, the daughter nearest the rosette was traced. If the daughters were equidistant, one was chosen at random.

Manual tracing with Volocity creates "track" measurements (see Fig. 9). Each track connects the 157 manually marked time points. Track length is the total distance migrated. Displacement is the shortest distance between the track start and endpoint. All measurements were calibrated to μm. An unpaired, 2-tailed, Student's T-test compared the mean values for near, far, and farthest cells traced in 14 rosette-ablated and 12 control embryos. Analyses and graphs were created with Microsoft Excel.

Pharmacological inhibition with cytochalasin D or rho-kinase

Embryos were incubated in 50% ASW with either Rho-kinase Inhibitor III (ROCKOUT, EMD4Biosciences, #555553) at a final concentration of 100 μM from a 50 mM DMSO stock or Cytochalasin D (Sigma) at a final concentration of 10 μM from a 1 mM DMSO stock. ROCKOUT is a specific ATP competitor with ROCK and this ROCKOUT concentration arrested wound-healing in mammalian epithelial cells (Yarrow et al., 2005). Fifty percent salinity lessens precipitation without affecting development (Table 1). Controls were subject to 50% ASW+DMSO. Drug incubation began at 8-cell or soccerball stage. For washout, embryos began treatment at soccerball and were removed at various time points and rinsed into control conditions (3 × 10 min with 50% ASW+DMSO). Prior to fixing, all embryos were washed 3 × 15 min in 100% ASW.

Table 1
Summary of embryo survival after ROCKOUT treatment at soccerball with and without drug washout.

	Total	Day 5	Hatching (%)	Rosette cells internalize?	Notes
Control	17	16	16/17 (94)	Yes	
Treated	20	0	0	No	All embryos are dead 72 h after treatment
Washout (3 h)	9	9	9/9 (100)	Delayed, but yes	All embryos survive and develop normally
Washout (8 h)	17	8	3/17 (18)	In 3, yes, after a delay. Otherwise, no	Some embryos at day 5 have gut and appendage development defects

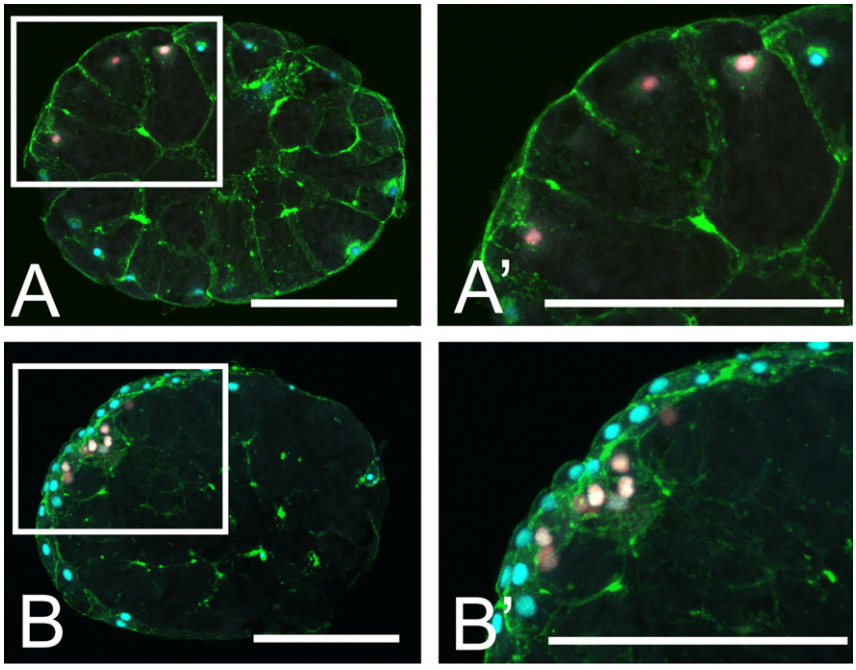

Fig. 3. Cells extrude yolk to the interior during gastrulation. Confocal projections through an 80 μm section of a pre-gastrulation embryo (12 hpf; A) and a post-gastrulation embryo (20 hpf; B). Rosette is labeled with dsRed-NLS (red nuclei). Actin (green) stained with phalloidin. Left, 10× view of the section. Area within the white box is pictured on the right (A′, B′). Scale bars are 100 μm.

Results

Rosette and epithelial sheet migration: germline internalizes second

To verify the timing of events during rosette internalization and to establish a baseline understanding of cell movement for later experiments, we performed lineage tracing with timelapse video. The timing of rosette formation and inward migration and the invariant lineage composition of the rosette are described in previous work (Gerberding et al., 2002; Browne et al., 2005; Price and Patel, 2008; Alwes et al., 2011). Briefly, rosette formation begins when Mav/g descendants begin to look more compact than their neighbors at approximately 12–14 hpf (Figs. 1 and 2; Alwes et al., 2011). This change in morphology may be explained by cell migration and yolk segregation to the center of the embryo (Alwes et al., 2011). Movement of the yolk out of cells to the interior of the embryo occurs through an as yet undetermined mechanism between soccerball and the onset of gastrulation (Browne et al., 2005; Alwes et al., 2011; Fig. 2). In *Orchestia*, yolk segregation is accomplished by superficial cleavage that lacks an S phase (Wolff and Scholtz, 2002). Although cell division occurs during this time period, yolk segregation to the center of the embryo is thought to account, at least in part, for the dramatic change in size of the cells pre- and post-gastrulation (Browne et al. 2005, Price and Patel, 2008; Fig. 3). Rosette internalization occurs when the rosette migrates inward and the epithelial sheet migrates toward the rosette. Internalization is in progress at 17 hpf at 26 °C (Fig. 1). By 20 hpf, the rosette is completely underneath the epithelial sheet (Fig. 1).

We add two observations to the previous research. First, the rosette and epithelial sheet both move toward one side of the embryo as the rosette internalizes (Fig.1). When viewed vegetally, the direction of migration is always away from the region occupied by precursors of the somatic mesoderm and endoderm. Thus, there are three components that overlap during the process of rosette formation and internalization: (1) yolk segregation, (2) the rosette migrates inward and the epithelial sheet undergoes epibolic movements, and (3) both the rosette and epithelial sheet move toward one side of the egg (summarized in Figs. 1 and 3).

Second, we find that the germline descendants internalize second, after the Mav descendants (Fig. 1, yellow in the schematic; Fig. 5). This directly conflicts with previous work and is further discussed below.

Bottle cells in Mav descendants, g internalizes separately

If the rosette is actively internalizing, then rosette cells should have cell-shape changes that are characteristic of migrating cells. To look for the presence of bottle cells in the rosette, we stained embryos and thick sections of embryos at the rosette stage for actin and/or tubulin. Descendants from g were distinguished from Mav by lineage tracing and g progeny's smaller size and distinctive tubulin staining (discussed below). During gastrulation, rosette cells have extruded most of their yolk and some Mav descendants exhibit bottle cell

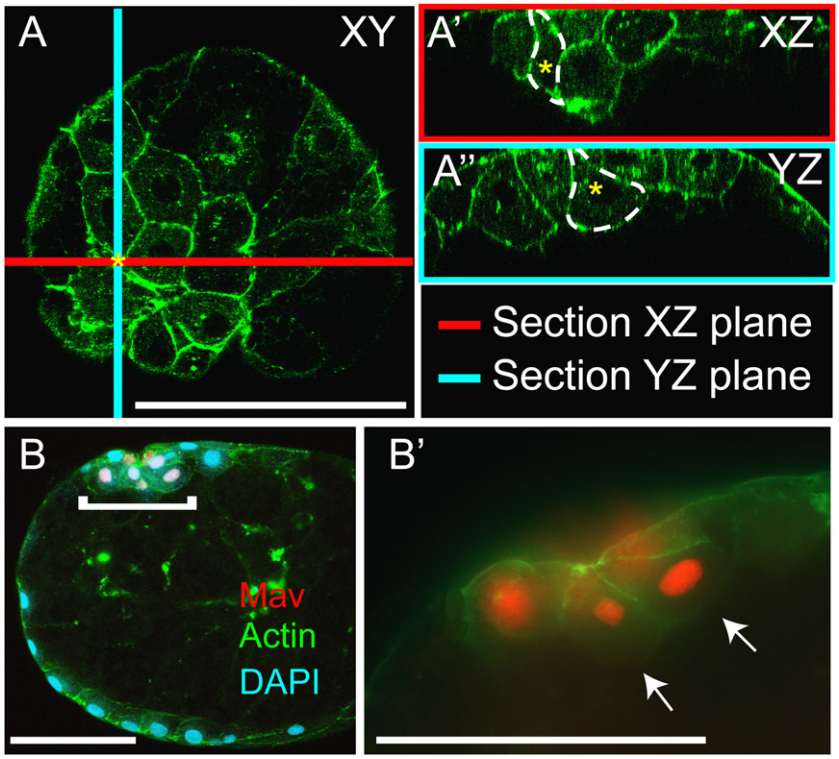

Fig. 4. Mav daughters exhibit bottle cell morphology during rosette internalization. (A–A′′) Confocal projection showing the rosette of an 18 h embryo stained with phalloidin (green). (A) XY section from a confocal projection. Red line marks XZ plane shown in A′, blue line marks YZ plane shown in A′′. Yellow asterisk marks the same cell in all panels. (B) Confocal projection of an 80 μm section through an 18 h embryo. Mav is labeled with dsRed-NLS (red nuclei). Area indicated by bracket is shown in B′. (B′) Fluorescent overlay of phalloidin stain (green) and dsRed-NLS (red). Arrows indicate bottle cells with an apico-lateral concentration of actin. Scale bars are 100 μm.

morphology (80% of embryos had bottle cells; $n=8/10$; Fig. 4). We confirmed that the bottle cells were Mav descendants by labeling Mav with dsRed-NLS at the 8-cell stage and then either creating optical sections with confocal microscopy (Fig. 4A) or using thick sectioning (Fig. 4B) to visualize cells at the rosette stage. Bottle cells also appear to have an apico-lateral concentration of actin and nuclei that are more toward the basal side of the cell (Fig. 4B′). It should be noted that the absence of bottle cells in some of the samples could be due to loss of the appropriate section and does not conclusively indicate a lack of bottle cells in those specimens.

Germline descendants in the 10 embryos were never observed to apically constrict at the rosette stage. Before gastrulation, g descendants are visible as a cluster at the edge of the rosette (Fig. 1; Fig. 5; Alwes et al., 2011). During gastrulation, we observed that g progeny migrate over the internalizing Mav cells and then move inward either randomly or as a group (Fig. 5A). We also found that, at the time of rosette formation, g descendants have long, tubulin-rich protrusions trailing from the edge of the cell away from the direction of migration (Fig. 5B; Extavour, 2005). Tubulin is a main component of the cytoskeleton, and this unique configuration of tubulin may indicate that it plays an important role in the mechanism of germline internalization. For the purposes of this study, we remained focused on the actin cytoskeleton.

Pharmacological inhibition of actin polymerization or of rho-kinase arrests gastrulation

The polarized assembly of microfilaments often enables cell migration (Ridley et al., 2003). We therefore expected the inhibition of actin polymerization to arrest gastrulation. We treated embryos with Cytochalasin D, which prevents the formation of microfilaments by binding to actin monomers (Goddette and Frieden, 1986). As expected, embryos that begin treatment at the soccerball stage never gastrulate. Instead, cells become disorganized and group together in “islands” that are cell clusters distributed around the egg ($n=15$; Fig. 6). Phalloidin staining reveals that microfilaments have lost organizational integrity and are choppy in comparison to controls. Moreover, the majority of cells have two nuclei, indicating incomplete cytokinesis, which is a phenotype linked to actin inhibition (Fig. 6).

The small GTP-ase *rho* and its downstream effectors are highly conserved molecular regulators of the cytoskeleton that enable acto-myosin contractility. In particular, *rho-kinase* is implicated in maintaining cell polarity and phosphorylating myosin across a variety of taxa (Riento and Ridley, 2003). If gastrulation in *Parhyale* is dependent on Rho-kinase, then inhibition of Rho-kinase should arrest gastrulation. We incubated embryos with the *rho-kinase* inhibitor ROCKOUT. ROCKOUT treatment at the 8-cell or soccerball stage arrests gastrulation. The rosette forms but never internalizes, and the embryo dies within 72 h of treatment (0% hatching; $n=14$ soccerball, $n=6$ 8-cell; Table 1).

We also performed washout experiments on embryos that were treated beginning at soccerball. If ROCKOUT is washed out after 3 h of treatment (approx. 15 hpf), all embryos recover and develop normally (100% hatching, $n=9$; Table 1). If the drug is washed out after 8 h of treatment (approx. 20 hpf), only 18% of embryos survive to hatching ($n=3/17$; Table 1) and ROCKOUT appears to irreversibly interfere with the apico-basal polarity and shape of epithelial sheet cells. Moreover, the cells of the rosette are not clustered together and only some have internalized ($n=12$, 8-cell; $n=8$, soccerball; Fig. 7; Table 1).

Mav and g can internalize independently

Although grouped together in the rosette, Mav and g descendants behave differently during gastrulation. If they are acting

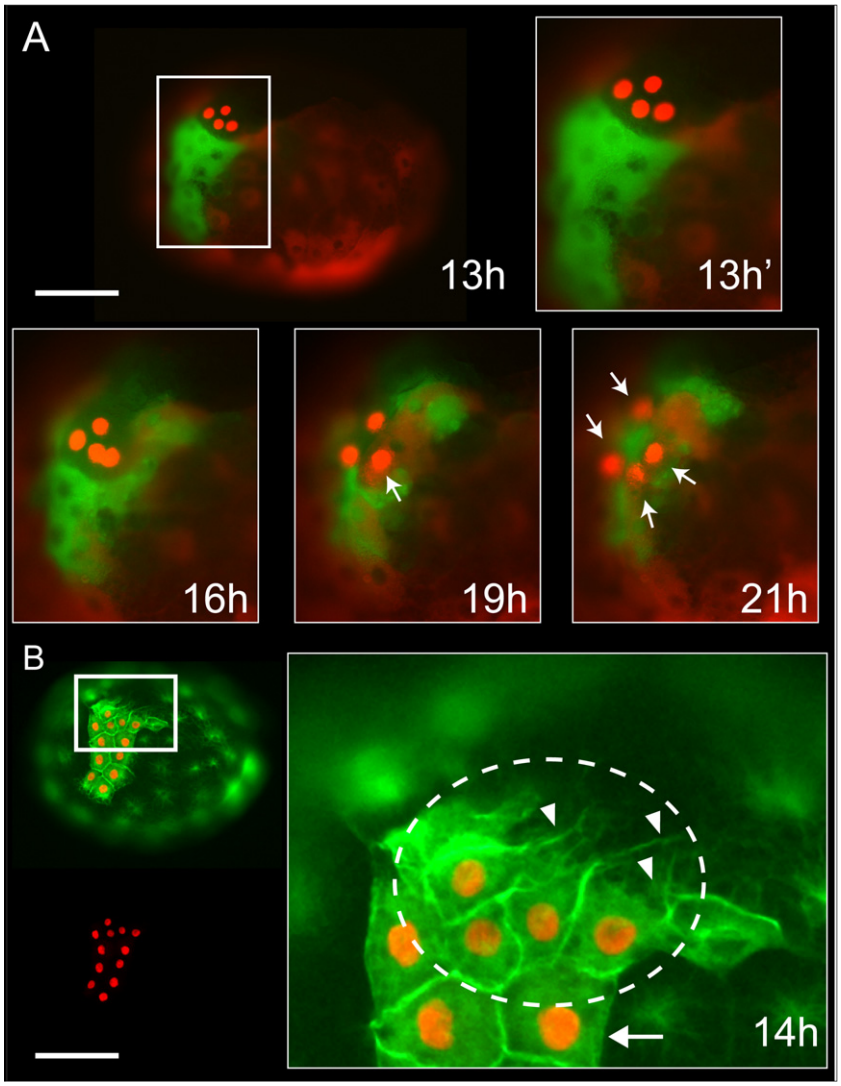

Fig. 5. The g-cells ingress separately from Mav cells (A) and have characteristic tubulin staining (B). (A) Stills from a timelapse video of gastrulation showing separate internalization of Mav daughters (FITC, green) and g daughters (dsRed-NLS, red nuclei) under the epithelial sheet (El, Er, and Ep daughters, TRITC, red). Focal plane remains at surface to illustrate internalization of g progeny. 13 h: Entire embryo at 13 hpf. 13 h–21 h: Area in white box in 13 h is shown throughout rosette internalization. By 16 h, the g daughters and the epithelial sheet are migrating over the Mav daughters. Arrows in 19 h and 21 h panels indicate germline cells that are completely underneath the epithelial sheet. (B) Approximately 14 hpf embryo with lineage tracer (dsRed-NLS, red nuclei) injected into Mav/g. Left, top: Overlay of tubulin (green) and dsRed-NLS. Left, bottom: dsRed-NLS expression. Area in white box is shown to the right. Right: The dotted line contains the g-lineage. Arrowheads indicate long tubulin fibers at one end of g-cells. Compare to the smooth border of a Mav cell (arrow). Scale bars are 100 μm.

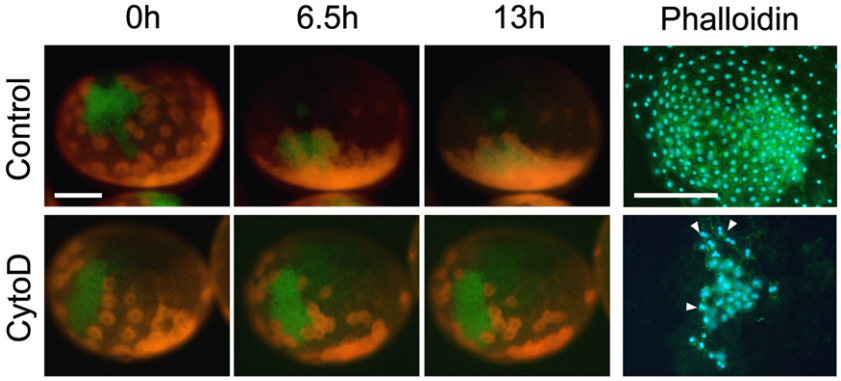

Fig. 6. Phalloidin treatment arrests gastrulation and interferes with the actin cytoskeleton. (Left) Stills from a timelapse video of untreated (top) and Cytochalasin D treated (bottom) embryos. Time is across the top, with the beginning of filming normalized to 0 h. Rosette and epithelial sheet were labeled with FITC (green) and TRITC (red). (Right) Cells from untreated (top) and Cytochalasin D treated (bottom) embryos stained with phalloidin at 20 hpf. Phalloidin is green, DAPI is blue. White arrowheads indicate cells with double nuclei. Scale bars are 100 μm.

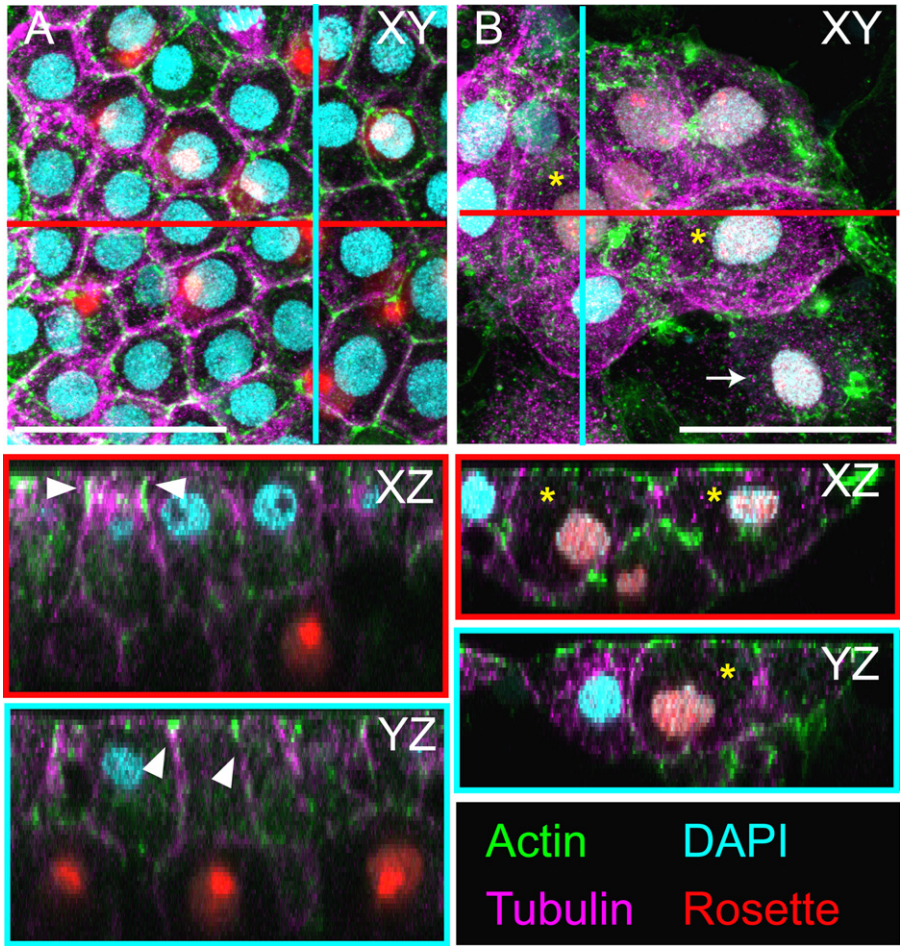

Fig. 7. Treatment with a Rho-kinase inhibitor during arrests development at gastrulation and affects normal epithelial morphology. Confocal images of rosette and epithelial cells in control embryos (A) and embryos subject to 8-hours of ROCKOUT treatment that were then washed into control conditions (B). Overlay of tubulin antibody (magenta), actin (phalloidin, green), rosette cells (dsRed-NLS, red nuclei), and nuclear staining (DAPI, cyan). Embryos are depicted 12 hours after the beginning of treatment; 4 h after the beginning of washout; 24 hpf. (A) Cells in the epithelial sheet are hexagonal and well-defined. Rosette cells are completely internalized. Arrowheads indicate putative cell–cell junctions. (B) Cells have lost all polarity and shape. Some rosette cells have internalized, but some remain on the surface. Red line in (A) and (B) indicates the position of the XZ section. Blue lines indicate the position of the YZ section. Yellow asterisks indicate rosette cells that are still at the surface and that appear in the alternate views XZ (red box) and YZ (blue box). Arrow indicates rosette cell that is not clustered with the others. Scale bar is 50 μm.

Table 2
Summary of ablation experiments and results.

Ablated region	Stage	Experiments[a]	Total[b] n	Results
Photoablation				
Entire rosette	Soccerball	6	14	Epithelial sheet migrates without the rosette
Entire rosette	8-cell	3	10	The ectoderm still aggregates into a germ disc without the rosette
Portion of Ep	Soccerball	1	3	Epithelial sheet migrates away from the ablated cells
Portion of El or Er	Soccerball	3	5	Epithelial sheet migrates away from the ablated cells
Leading edge	Soccerball	3	6	Rosette internalizes, epithelial sheet movement shows a range of phenotypes
g	Soccerball	4	10	Mav internalizes normally
g	8-cell	3	8	Mav internalizes normally
Manual ablation				
Mav	8-cell	2	6	g internalizes and migrates

[a] Number of experiments containing the embryos that were pooled to generate the "Total n."
[b] Final number of embryos included in analysis.

independently, ablation of either population should not affect internalization of remaining cells. Previous work found that manual ablation of g at the 8-cell stage does not affect gastrulation, and that normal development can still occur despite photoablation of any of the mesoderm precursors (ml, mr, or Mav) (Price et al., 2010; Alwes et al., 2011). We confirmed that photoablation of g at the 8-cell or soccerball stages did not prevent normal migration and internalization of Mav (Table 2). To test whether manual ablation of Mav has an effect on internalization of g, we manually ablated Mav at the 8-cell stage ($n=6$). Here, observation of g migration during gastrulation was difficult due to the high mortality of embryos when filming and/or photography was attempted in addition to manual ablation. However, of the embryos that survived to appendage formation, the germline does reach its normal position late in

development as confirmed by antibody staining for the germline marker Vasa ($n=3$; representative embryo in Fig. 8). In normal embryos, g descendants appear as a cluster in the center of the developing germ band that then splits into two bilaterally symmetric groups as the cells migrate to their final location within the somatic gonads (Gerberding et al., 2002; Browne et al., 2005, Fig. 8).

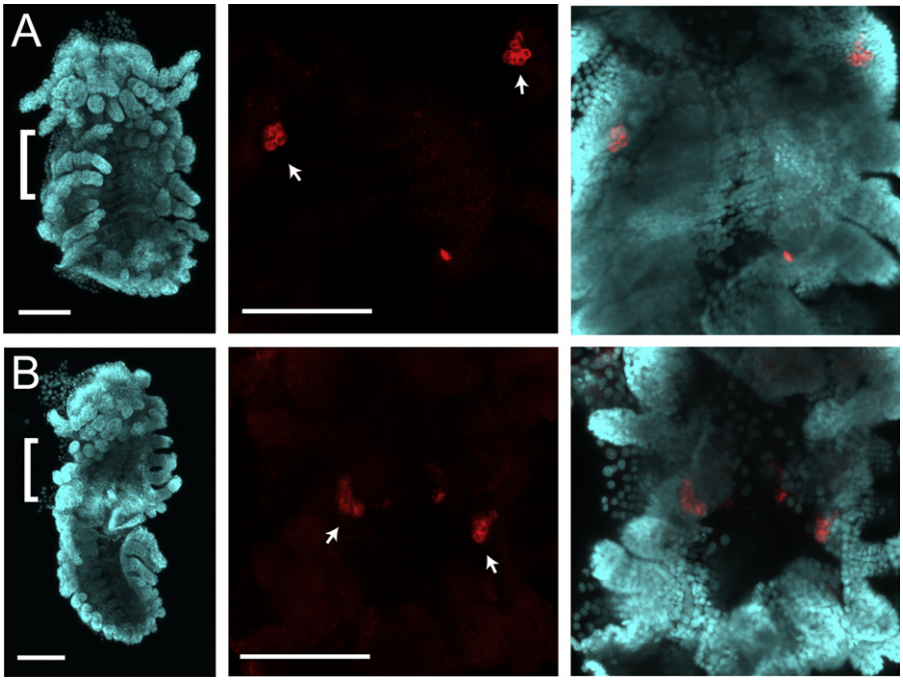

Fig. 8. The germline arrives at its normal location when Mav is manually ablated. Confocal images of late appendage development (S21) embryos that were either unperturbed (A) or had Mav manually ablated (B). Nuclei are in blue (DAPI) and the germline marker Vasa is in red. Left panel shows ventral view of the entire embryo, anterior to the top. Bracket indicates the approximate area that is shown in the two right panels. Middle is Vasa stain. Right is overlay of DAPI and Vasa. In both animals, the germline is found in two bilaterally symmetric clusters (arrows in middle view), as expected. Scale bars are 100 μm.

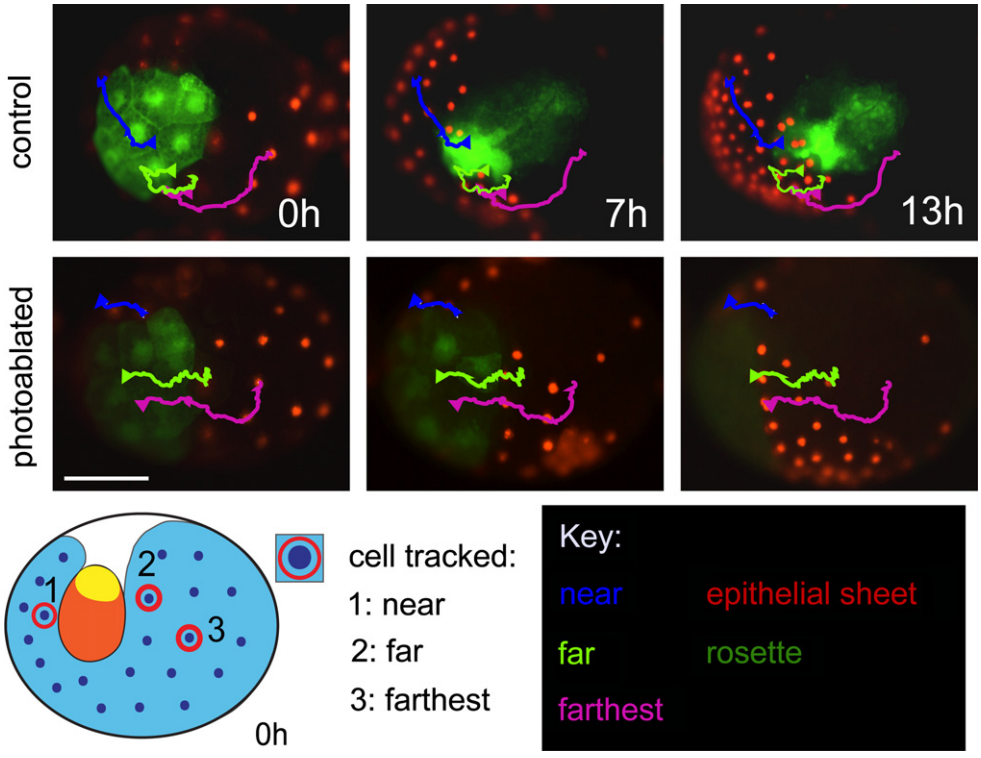

Fig. 9. Cell tracking in the epithelial sheet when the rosette is ablated gives tracks of similar length between control and ablated embryos. Stills of a representative control (top) and photoablated (bottom) embryo from a timelapse video superimposed with tracks generated from connecting 157 manually labeled time points of the migration of near (blue), far (bright green), and farthest (pink) cells. Triangle indicates the endpoint of migration. Time is shown in hours and is normalized to 0 h at the beginning of cell tracking. Stills are oriented so that the direction of rosette and epithelial sheet migration is to the left. Lower left: Schematic of a vegetal view of a 13 hpf embryo (approximate stage normalized to 0 h in the video). A red circle indicates examples of cells chosen for tracking. 1: near, 2: far, 3: farthest. Rosette is labeled with FITC (green) and the epithelial sheet is labeled with TRITC (red). Scale bar is 100 μm.

Rosette and epithelial sheet migration are autonomous: ablation of the rosette and the leading edge of the epithelial sheet

If rosette internalization depends on cooperative behavior between the rosette and epithelial sheet, then ablation of either population should arrest gastrulation. When the rosette is photoablated just before gastrulation, cells in the epithelial sheet do not exhibit significant differences in migration length or overall displacement as compared to controls ($n=14$ ablated, $n=12$ control; Figs. 9 and 10). *P*-values for all migration length comparisons were insignificant (near: 0.47, far: 0.42, farthest: 0.71). *P*-values for displacement comparisons were also insignificant (near: 0.31, far: 0.16, farthest: 0.10). We did observe that migrating epithelial sheet cells in control embryos turn toward the rosette, whereas cells in photoablated embryos travel in a relatively straight line (Fig. 8). In addition, the epithelial sheet appears to condense normally.

When the rosette (Mav+g) is photoablated at the 8-cell stage, approximately 8-hours prior to epithelial sheet formation, a normal-looking germ disc still forms ($n=10$; Fig. 11; Table 2). Confocal images of these embryos reveal that the ectodermal precursors appear to condense and migrate normally (Fig. 11).

We performed two additional ablations as controls (Table 2; Fig.12). There is ample evidence in the literature that when an epithelium is scratched, cells adjacent to the wound can migrate to close it in a wound-healing response (for review see Martin and Parkhurst, 2004). To test whether cell ablation triggers a

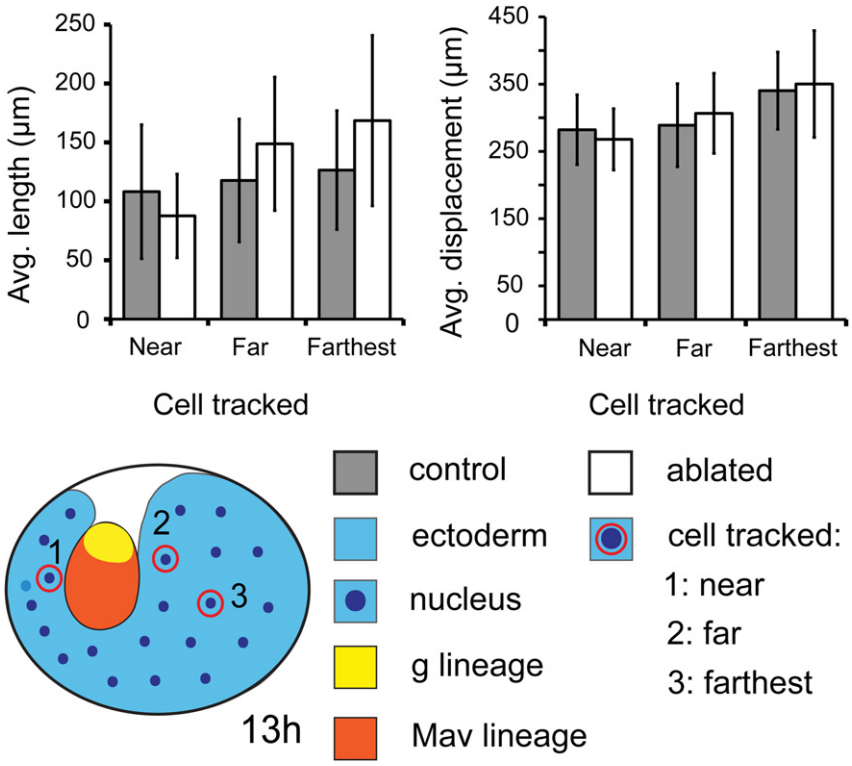

Fig. 10. Photo-ablation of the rosette just prior to gastrulation has no significant effect on migration of the epithelial sheet. Top: Graphs showing the average migration length and average displacement of cells in the epithelial sheet in control (non-ablated; $n=12$) and ablated ($n=14$) groups. See methods and materials for further detail. Error bars indicate standard deviation. Difference is not significant in either the length migrated (left) or the displacement of cells (right) (p-value >0.05 in each case). Bottom: Schematic of a vegetal view of a 13 h embryo. Red circle indicates examples of cells chosen for tracking. 1: near, 2: far, 3: farthest.

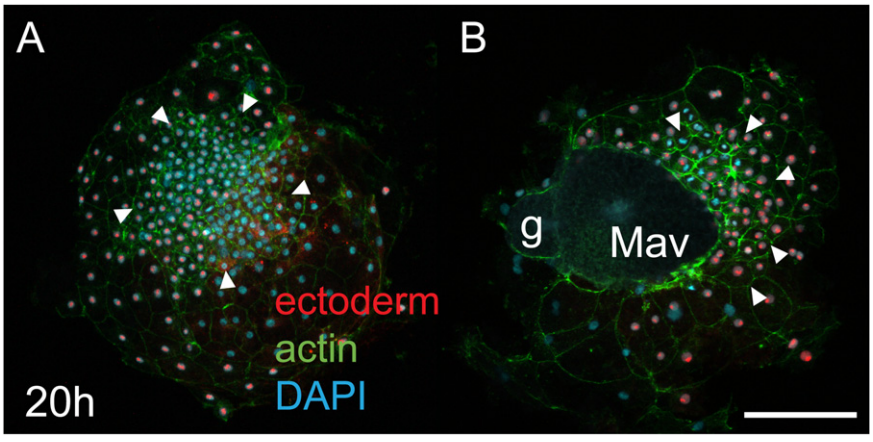

Fig. 11. Ablation of the rosette at the 8-cell stage does not hinder migration of the epithelial sheet. A: Confocal stack of a control embryo at 20 hpf. B: Confocal stack of an embryo with Mav and g photoablated at the 8-cell stage. The remains of Mav and g are clearly visible. Arrowheads indicate area where epithelial sheet cells that have condensed and migrated. El or Er injected with TRITC (red) and El, Er, and Ep injected with dsRed-NLS (red nuclei). Nuclei in blue (DAPI), actin in green (phalloidin).

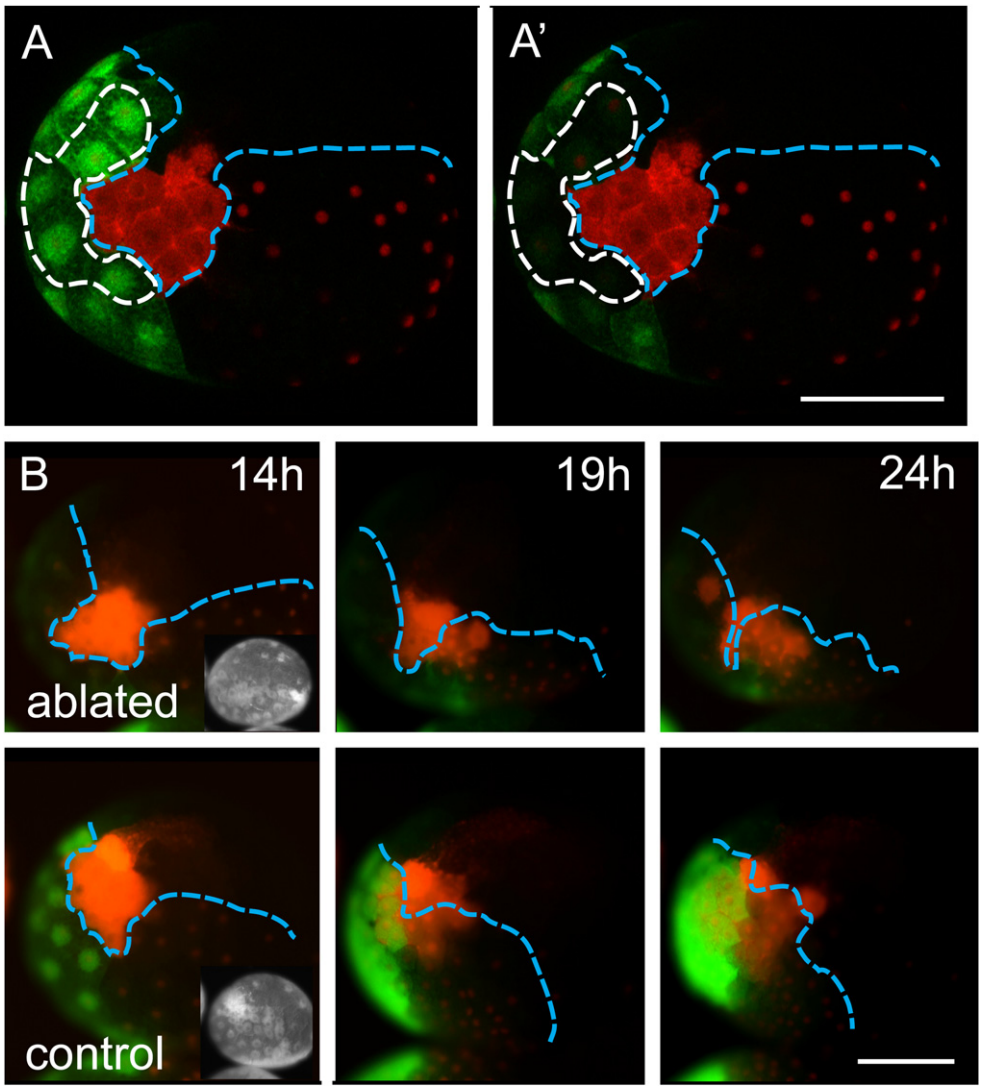

Fig. 12. Ablation of a portion of the epithelial sheet adjacent to the rosette does not affect rosette internalization. Confocal projections of a 13 hpf embryo before (A) and after (A′) confocal ablation. White dotted line indicates the region targeted for ablation. Note photobleaching from A to A′. Blue dotted line indicates approximate epithelial sheet boundary. Rosette labeled with TRITC (red), El progeny labeled with FITC (green), Er and El progeny labeled with dsRed-nls (red nuclei). (B) Stills from a timelapse video of ablated (top) and control (bottom) embryos. Stills are focused on a single embryo and rotated to place the direction of rosette and epithelial sheet migration to the left. Inset shows brightfield view just before the beginning of filming. Scale bar is 100 μm.

wound-response in the epithelial sheet, we ablated a portion of the epithelial sheet adjacent to the rosette ($n=6$; Fig. 12; Table 2) or a portion of epithelial cells at a distance from the rosette (i.e., descendants of Ep) ($n=3$; Table 2) and filmed embryos as we did for rosette ablation experiments. When we ablated a portion of the epithelial sheet adjacent to and roughly the same size as the rosette, the rosette internalized normally and the remaining epithelial cells migrated to cover the rosette but not the ablated area (Fig. 12B). When we ablated a portion of Ep cells, the remaining epithelial sheet cells migrated away from the dead cells. In each case, the remaining cells of the epithelial sheet did not obviously change their migration paths to compensate for the ablated cells. Taken with the observation that epithelial cells travel in a straight line and do not migrate to cover an ablated rosette, these results indicate that epithelial sheet migration when the rosette is ablated is not a response to wounding.

When the leading edge of the epithelial sheet is ablated, the rosette is able to internalize. Because ablation of the entire epithelial sheet just before gastrulation would likely be a lethal ablation, we focused our attention on the epithelial sheet cells touching the rosette. This leading edge of cells is the most likely candidate for any interaction between the rosette and epithelial sheet because it comprises the first cells to cover the rosette.

When the leading edge of epithelial cells is killed just before gastrulation, condensation and inward migration of the rosette slows but occurs normally (Fig. 13). However, ablation of the leading edge results in various phenotypes in the remaining epithelial sheet cells (Figs. 13 and 14). In some cases ($n=2/6$, 33%), the dead leading edge cells were absorbed into the embryo and the epithelial sheet condensed normally (Fig. 13). In the majority of cases ($n=4/6$, 66%) at least one row of ectodermal cells behind the ablated leading edge failed to condense and migrate and instead retained its yolky, pre-migration size and phenotype. In addition, in these embryos it appeared that the rosette remained at the point of internalization rather than migrating to one side of the embryo (Fig. 14).

Discussion

To summarize, we found that each lineage in the rosette exhibits unique cellular behaviors during rosette internalization, that the internalization of the rosette can be blocked by treatment with

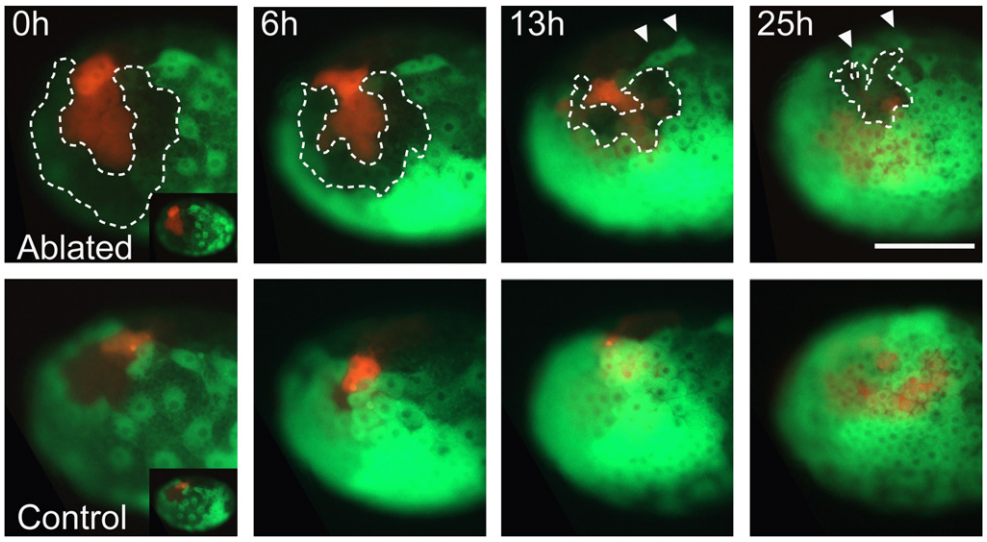

Fig. 13. Rosette internalization slows, but still occurs when the leading edge is ablated. Stills from a timelapse video of an embryo with the leading edge of ectoderm ablated (top) and a microinjected but unablated control (bottom). The beginning of the film is normalized to 0 h. White dotted line outlines areas of dead, photoablated cells that are visible as the rosette internalizes. Arrowheads indicate ectodermal cells that migrate around the dead cells to close the epithelial sheet as the rosette internalizes. Rosette is labeled with TRITC (red), and the epithelial sheet is labeled with FITC (green). Scale bars are 100 μm.

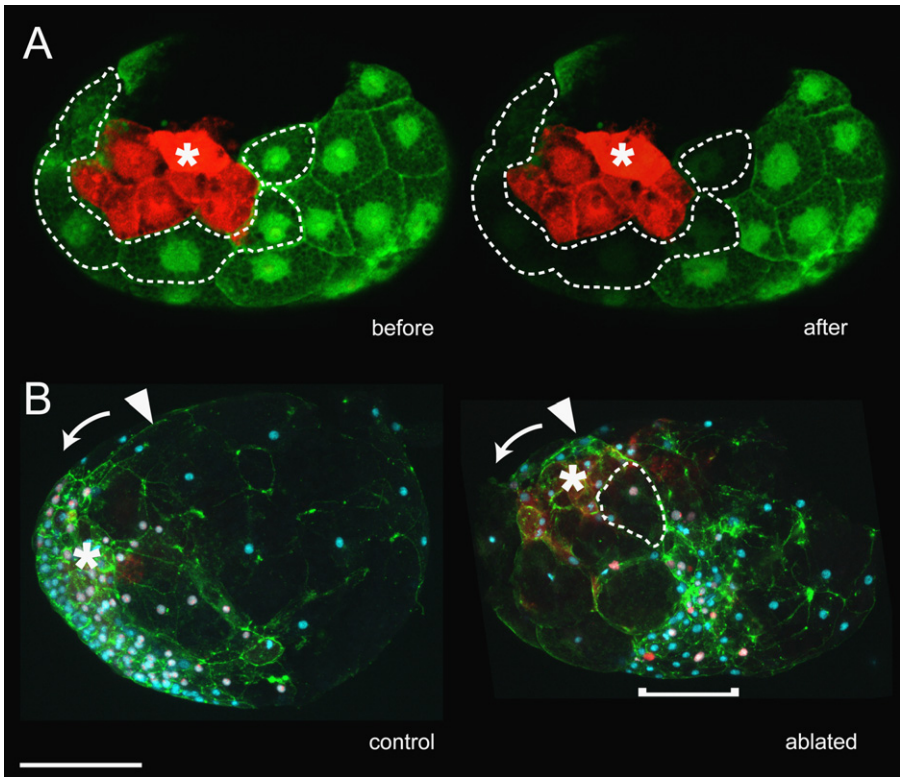

Fig. 14. Photoablation of the leading edge of the epithelial sheet can result in impaired epithelial sheet and rosette condensation and migration. A: Confocal projections of the vegetal view of a S6 embryo before and after photoablation. Embryo is the ablated embryo in B. Dotted line indicates region specified for laser scanning, note that this area is photobleached in the second image. Rosette labeled with TRITC, (red); El, Er labeled with FITC, green and ds-red-NLS (nuclei not visible in this view because of TRITC brightness). Asterisk indicates g-lineage, which marks the edge of the rosette and has a higher concentration of TRITC because it divides less. (B) The rosette internalizes, but does not migrate to one side of the embryo. Confocal projections showing lateral views of a fixed control and ablated embryo stained for actin (green) and nuclei (blue) at 30 hpf. Ablated embryo is the same embryo as in A. Mav/g is labeled with TRITC (red haze, white asterisk) and El and Er progeny are labeled with dsRed-NLS (red nuclei). Small white arrowheads indicate approximate internalization site of the rosette. Arrow indicates direction of normal migration. In the ablated embryo, the rosette internalizes but does not migrate. Dashed line outlines an ectodermal cell that did not condense properly. Bracket indicates some ectodermal precursors that were able to migrate and condense.

Cytochalasin D or Rho-kinase, and that the rosette and the epithelial sheet act independently during early gastrulation as shown by the reciprocal ablation and observation of the rosette and adjacent epithelial sheet cells.

Independent sub-populations within the rosette

Although grouped together in the rosette, we show that Mav and g descendants behave independently and are not following a

broad "rosette" program during gastrulation. We observed that Mav cells have bottle cells, but that g descendants do not and can migrate inward independently of Mav cells (Figs. 4 and 8). Specifically, we observed that g progeny internalize and migrate to their final location despite manual ablation of Mav at the 8-cell stage (Fig. 8). How g internalizes when Mav is ablated remains unknown. It is possible that g migration during gastrulation is abnormal when Mav is absent, but that g progeny still arrive at their expected location by the time appendages have formed. In our hands, manual ablation of Mav in addition to lineage tracing g progeny through microinjection and timelapse video or photography resulted in high embryo mortality, and we were unable to make conclusive observations about the path of g progeny migration during gastrulation in Mav-ablated embryos. In addition, inhibition of Rho-kinase completely prevents rosette internalization (discussed below; Table 1). In our washout experiments, however, some cells do manage to internalize after prolonged Rho-kinase treatment followed by washout (Fig. 7). It is possible that these cells reflect different internalization mechanisms in Mav vs. g descendants. In this study, we did not distinguish between the two populations during drug treatment. Future experiments on the migration of the *Parhyale* germline could use immunohistochemistry and a time-course of development during germline migration in control and Mav-ablated animals. Further work with Rho-kinase could also include differentiating between Mav and g daughters to discern its role in each lineage. These studies could also focus on microtubules as potentially important to germline migration given their unique formation in g progeny (Fig. 5; Extavour, 2005).

Our observation that the germline migrates inward after Mav descendants (Fig. 5), directly conflicts with Alwes et al. (2011) and is inconsistent with gastrulation in *Orchestia* (Wolff and Scholtz, 2002), but agrees with Price and Patel (2008). This conflict may be a result of differing methodology; Price and Patel (2008) and this study injected lineage tracers, but Alwes et al. (2011) tracked cells in brightfield. Fluorescent labeling (used here) may make it easier to determine the precise period when a cell loses contact with the surface as we can visualize the entire cell, including extensions from the cell body. Alternatively, the injection of lineage tracers could cause cells to behave differently during development, although other studies in crustaceans have used fluorescent lineage labeling without the apparent generation of such an artifact (Wolff and Scholtz, 2002). Finally, it may be that the lab-raised populations used in each *Parhyale* study differ from each other. The last two of these alternatives would suggest that the order of internalization of Mav and g progeny is flexible and does not affect later development.

That the germline behaves independently may not be unusual as primordial germ cells in a variety of organisms such as *Drosophila,* zebrafish, and mice have specialized and unique motility that can manifest at a variety of developmental stages to allow them to reach their final positions in the somatic gonads (reviewed in Molyneaux and Wiley (2004)). Internalization of the germline and the adjacent anterior mesoderm is also decoupled in *Orchestia*, where the germline first sinks into the yolk and the mesoderm internalizes later through a blastoporal groove (Wolff and Scholtz, 2002). Although a detailed mechanistic study of gastrulation in *Orchestia* remains to be done, it is possible that the germline and mesendoderm in *Orchestia* exhibit different cell behaviors as they internalize.

Actin or rho-kinase inhibition prevents gastrulation

The presence of bottle cells in the rosette in combination with the result that pharmacological inhibition of actin polymerization or Rho-kinase activity prevents normal rosette internalization (Figs. 6 and 7) provides evidence for ingression or invagination. Furthermore, these results suggest that apical constriction may be the mechanism of internalization for Mav descendants. As expected, inhibiting the actin cytoskeleton arrests gastrulation in *Parhyale* (Fig. 6). Rosette cells remain on the surface, and the ectodermal precursors appear to lose epithelial integrity and do not migrate. It is interesting to note that the rosette cells remained adjacent to each other over the course of filming in all treated embryos. This is probably due to their more compact nature and their proximity, but could also point to a difference in function of the actin cytoskeleton in the rosette vs. the epithelial sheet. For example, the primary function of actin in the rosette may be to move it inward through something like apical constriction, whereas in the epithelial sheet actin may primarily function in cell–cell adhesion.

Inhibiting Rho-kinase in *Parhyale* gastrulation can irreversibly interrupt normal cell polarity (Fig. 7), which may negatively affect a variety of cell migration processes including normal migration of the epithelial sheet, apical constriction in Mav, and/or the extension of filopoda from motile cell populations. Our washout experiments suggest Rho-kinase must be available during rosette internalization. If the drug is washed out at 15 hpf, as the rosette is forming and beginning to internalize, 100% of embryos are able to recover (Table 1). However, if embryos are treated over the course of rosette internalization and then the drug is washed out after rosette internalization was supposed to finish (20 hpf), survival reduces to 18%. Rho-kinase acts downstream of a variety of known cell polarity pathways including non-canonical wnt-signaling (the planar cell polarity pathway) during wing, eye, and salivary gland development in *Drosophila* (Mizuno et al., 1999; Winter et al., 2001; Riento and Ridley, 2003; Xu et al., 2008). Components of this pathway, such as Frizzled, Disheveled, and PAR proteins, are highly conserved and are attractive candidates for study in *Parhyale*.

Previous work has mentioned ingression and invagination as the major cell behaviors that occur in the rosette during internalization (Gerberding et al., 2002; Browne et al., 2005; Price and Patel, 2008). At the cellular level, the main distinguishing factor between the two behaviors is their relationship with neighboring cells. In *Drosophila,* the invaginating cells remodel their cell–cell junctions as they apically constrict (Martin et al., 2009). Pulsed contractions of an acto-myosin meshwork that is continuous between the apically constricting cells and their neighbors then buckles the epithelium, creating multiple tissue layers through folding (Martin et al., 2010). In contrast, ingressing cells in sea urchin gastrulation lose their cell–cell junctions, apically constrict, and then migrate to the interior. Neighboring cells then move to close the gap that is left behind (Fink and McClay, 1985; Wu et al., 2007). Both behaviors are associated with bottle cells because apical constriction can provide the force for epithelial bending and/or for the initial movements of a cell or a small group of cells to the interior. Future work with *Parhyale* could focus on cell-to-cell junctions during gastrulation to definitively distinguish between ingression and invagination.

The rosette and the epithelial sheet move independently during rosette internalization

We found no evidence that the either the rosette or the epithelial sheet relied upon an inductive signal from the opposite population or was emitting an inductive signal necessary for the gastrulation behavior of the opposite group. In our experiments, the epithelial sheet migrated the same distance regardless of whether viable rosette cells were present or had been photoablated just before gastrulation (Figs. 9 and 10). Rosette internalization also progresses in the absence of a viable leading edge

of epithelial sheet cells (Figs. 13 and 14). These results suggest that the cue for migration and condensation of the epithelial sheet is not an inductive signal from the rosette, but is intrinsic to ectodermal precursors. We did observe that the rosette might have some directional control over the migration path of epithelial sheet cells. When the rosette is ablated, epithelial sheet cells migrate in a straight line instead of turning toward the position of the rosette (Fig. 9). Aside from the change in direction, epithelial condensation was unaffected (Fig. 10). It may be that ectodermal cells were physically unable to turn because of the lingering cellular debris from the dead rosette cells. When, as in our experiments where the rosette is ablated at the 8-cell stage, cellular debris from dead cells are extruded or absorbed, the epithelial sheet still forms a normal-looking epithelial germ disc (Table 2, Fig. 11). Because the 8-cell ablation takes place several hours before any putative signaling event, this supports our conclusion that the formation and migration of the epithelial sheet is independent of the rosette.

One caveat to the independence of the rosette and the epithelial sheet is that we observed that ablation of the leading edge of ectodermal cells affects the migration of the internalizing rosette to one side of the embryo and that it can also interfere with condensation and migration of the epithelial sheet (Fig. 14). Because the rosette migrates inward but does not migrate to one side when the leading edge is ablated, internalizing and moving to one side appear mechanistically distinct. The most straightforward explanation is that the cellular debris from dead leading edge cells prevents the condensation of neighboring epithelial sheet cells and, ultimately, the post-internalization migration of the rosette. The presence of some properly condensed ectodermal cells at the posterior-most end of the epithelial sheet implies that those cells have enough distance from the cellular debris of the leading edge to be unaffected (Fig. 14).

When we ablated portions of the epithelial sheet as controls for our rosette ablations, however, we never observed failure of neighboring epithelial cells to condense and migrate (Fig. 12). This could be due to the smaller number of cells ablated, or an alternative scenario is that the leading edge of the epithelial sheet induces or enables post-internalization migration of the rosette and/or condensation and migration of the remaining epithelial sheet cells. Based on lineage tracing, all of the cells we ablated were descendants of El and Er. It is possible that the cells in the leading edge have cell-lineage specific signals. The posterior, properly condensed cells may therefore be evidence for signaling among Ep daughters. Given this scenario, we hypothesize that yolk segregation may play a vital role in normal gastrulation. When the leading edge of the ectoderm is killed, those cells cease to divide and fail to extrude their yolk to the interior. This may set up a physical barrier that prevents the post-internalization migration of the rosette and yolk extrusion/migration of other cells, or the act of extruding the yolk may itself be the motor for pushing cells to one side of the embryo.

That the epithelial sheet and the rosette move independently is consistent with previous work suggesting that the instructions for early gastrulation movements are provided through maternal determinants that are segregated via specialized cytoplasm (Extavour, 2005; Alwes et al., 2011). When 8-cell blastomeres are independently cultured, Extavour (2005) showed that the germline marker *Vasa* is always expressed in the portion of the embryo that will give rise to germline. Alwes et al. (2011) performed 8-cell micromere ablations and brightfield lineage tracing to show that remaining blastomeres migrate normally through early gastrulation in the absence of ml, en, and g progeny. Independent gastrulation movements also support results showing that 8-cell blastomeres are capable of replacing each other within mesoderm and ectoderm "equivalency" groups (Price et al., 2010). Briefly, ablation of a mesodermal blastomere (ml, mr, or Mav) triggers compensation from the remaining mesodermal blastomeres and ablation of an ectodermal cell (El, Er, or Ep) can trigger replacement from the remaining ectoderm cells, but neither will a mesoderm cell compensate for an ablated ectoderm cell nor ectoderm for mesoderm. In these compensation studies, different aggregations of cells appear to work together to the exclusion of neighboring populations of cells. The same appears true for different populations of cells during gastrulation.

Our results for the epithelial sheet differ from the scenario suggested by Alwes et al. (2011), in which the internalization of the rosette is autonomous but the epibolic movements of the epithelial sheet are non-autonomous. In their model, cell–cell contact between the rosette and the epithelial sheet is required for cell–cell signaling that controls the epibolic movements of the epithelial sheet. Our results suggest that the epithelial sheet is able to move without contact with viable rosette cells. Instead, the required cell–cell contact appears to be between the leading edge of the epithelial sheet and the ectodermal precursors that are one row behind the leading edge.

Future work could focus on potential molecular signaling mechanisms to investigate the role of the leading edge of the epithelial sheet. *Drosophila* dorsal closure is a well-understood invertebrate example of an epithelium with a leading edge that influences morphogenesis. In this case, the leading edge of the epidermis forms a contractile acto-myosin "purse string" that participates in the migration of the epidermis over the amnioserosa (Young et al., 1993; Kiehart et al., 2000). The TGF-b signaling factor decapentaplegic (dpp), Jun-Kinase (JNK) signaling, and apical constriction in the amnioserosa have also been implicated in normal dorsal closure (for review, see Harden (2002) and Jacinto et al. (2002)). Interestingly, in this example, as in *Parhyale*, neither population of cells (the amnioserosa and epidermis in *Drosophila,* or the rosette and epithelial sheet in *Parhyale*) is absolutely necessary for continued migration of the other population (Kiehart et al., 2000).

Final thoughts

Scholtz and Wolff (2002) posited a list of potentially apomorphic developmental traits that further delineate amphipods as a monophyletic clade. Among these is gastrulation through an anterior gastrulation center, which is the case in *Parhyale*, *Orchestia*, and several other amphipod species (reviewed in Gerberding and Patel (2004)). Whether the mechanism of cell internalization through the gastrulation center is conserved across these taxa remains unknown. *Orchestia* and *Parhyale* exhibit similar cell cleavage, fate, and lineage patterns (Scholtz and Wolff, 2002; Gerberding and Patel, 2004; Alwes et al., 2011). In *Orchestia*, gastrulation progresses in three phases, two of which share marked similarities with *Parhyale* gastrulation (Wolff and Scholtz, 2002; Scholtz and Wolff, 2002; summarized in Gerberding and Patel (2004) and Alwes et al. (2011)). First, yolky cells migrate to the interior to form vitellophages. There is no corresponding phase in *Parhyale.* Second, a sickle-shaped group of ectodermal precursors surround the mesendoderm and germline. The mesendodermal cells and the germline cells originate from 8-cell blastomeres that correspond to Mav and g in *Parhyale*, and they form the gastrulation center. Gastrulation begins when the germline sinks into the yolk and is overgrown by epibolic movements of the presumptive ectoderm to form the germ disc. This second phase shares features with *Parhyale* rosette internalization. Finally, the mesendoderm in *Orchestia* internalizes through a blastoporal groove and the somatic mesoderm internalizes at the edges of the germ disc. This third phase of *Orchestia* gastrulation is similar to the second phase of *Parhyale* gastrulation where the

somatic mesoderm and endoderm internalize at the periphery of the germ disc (Gerberding et al., 2002; Price and Patel, 2008). It would be rewarding to investigate whether bottle cells also appear in the immigrating mesendoderm and whether the germline in each species shares a mechanism for internalization. Further studies into the mechanism of cell internalization among amphipods would inform our knowledge of the plasticity of early gastrulation strategies among crustaceans.

Why the *Parhyale* rosette forms a distinct structure despite being comprised of independently acting cell populations remains an open question. The rosette does not appear to have inductive abilities, which makes it a different structure than the arachnid cumulus. The rosette does, however, initiate gastrulation, and Mav and g are sister blastomeres. One possibility for the formation of the rosette is that the necessary changes in cell morphology that lead up to gastrulation such as yolk segregation must occur earlier in the first populations to internalize and migrate. Mav and g descendants internalize early and around the same time, and so must undergo yolk segregation before adjacent epithelial cells. Soon thereafter, the epithelial sheet cells farthest from the rosette must begin migrating in order to reach the condensing germ disc. These cells are the next to segregate their yolk and migrate. Changes in morphology then progress from the cells of the rosette toward the far edge of the epithelial sheet and from the far edge of the epithelial sheet toward the rosette until gastrulation is complete. The distinctness of the rosette and the epithelial sheet may therefore reflect heterochrony in yolk segregation during gastrulation. This idea is consistent with the findings of Alwes et al. (2011), who describe that micromere descendants are the first to migrate and compact at the beginning of rosette formation after the soccerball stage.

In addition, our results suggest that yolk segregation may play an important role in early *Parhyale* development. The amount and location of yolk during embryogenesis has a profound influence on the evolution of development. For example, sea urchins in the genus *Heliocidaris* display both planktotrophic larva (*Heliocidaris tuburculata*) and lecithotrophic larva (*Heliocidaris erythrogramma). H. tuburculata* gastrulates like the classic example *Strongylocentrotus purpuratus*: through ingression of the primary mesenchyme and invagination of the gut. In contrast, presumably to accommodate a large amount of yolk, the embryos of *H. erythrogramma* elongate and internalize their gut tissue through involution (Wray and Raff, 1991). Not only does yolk present a bulky obstacle around which cells must migrate, it can also serve as an important substrate. In *Drosophila*, interaction with the yolk sac is necessary for survival of the amnioserosa during germ band retraction and dorsal closure (Reed et al., 2004). How the yolk influences and contributes to cell behavior during gastrulation in amphipods may be a crucial part of understanding cellular morphogenetic movements and their evolution among arthropods.

Acknowledgments

We would like to thank S. Black, J.-Y. Lee, P. Liu, M. Modrell, and M. Protas for insightful edits. S. Haigo and J.-Y. Lee also provided advice and help with experiments. We would also like to thank two anonymous reviewers for comments that greatly improved the manuscript. R.C. Chaw was supported by an NSF pre-doctoral fellowship.

References

Akiyama-Oda, Y., Oda, H., 2003. Early patterning of the spider embryo: a cluster of mesenchymal cells at the cumulus produces dpp signals by germ disc epithelial cells. Development 104, 391–402.

Akiyama-Oda, Y., Oda, H., 2006. Axis specification in the spider embryo: dpp is required for radial to axial symmetry transformation and sog for ventral patterning. Development 133, 2347–2352.

Alwes, F., Hinchen, B., Extavour, C.G., 2011. Patterns of cell lineage, movement, and migration from germ layer specification to gastrulation in the amphipod crustacean *Parhyale hawaiensis*. Dev. Biol. 359, 110–123.

Anderson, D., 1973. Embryology and Phylogeny in Annelids and Arthropods. Pergamon, New York.

Browne, W.E., Price, A.L., Gerberding, M., Patel, N.H., 2005. Stages of embryonic development in the amphipod crustacean, *Parhyale hawaiensis*. Genesis 42, 124–149.

Davidson, L.A., 2008. Integrating morphogenesis with underlying mechanics and cell biology. Curr. Top. Dev. Biol. 81, 113–133.

Dawes-Hoang, R.E., Parmar, K.M., Christiansen, A.E., Phelps, C.B., Brand, A.H., Wieschaus, E.F., 2005. Folded gastrulation, cell shape change and the control of myosin localization. Development 132, 4165–4178.

Extavour, C.G., 2005. The fate of isolated blastomeres with respect to germ cell formation in the amphipod crustacean *Parhyale hawaiensis*. Dev. Biol. 277, 387–402.

Fink, R.D., McClay, D.R., 1985. Three cell recognition changes accompany the ingression of sea urchin primary mesenchyme cells. Dev. Biol. 107, 66–74.

Foelix, R.F., 1996. The Biology of Spiders, 2nd ed. Oxford Thieme, New York.

Gerberding, M., Patel, N.H., 2004. Gastrulation in crustaceans. In: Stern, C.D. (Ed.), 2004. Gastrulation: From Cells to Embryo, 1st ed. Cold Spring Harbor Laboratory Press, New York, pp. 79–84.

Gerberding, M., Browne, W.E., Patel, N.H., 2002. Cell lineage analysis of the amphipod crustacean *Parhyale hawaiensis* reveals an early restriction of cell fates. Development 129, 5789–5801.

Goddette, D.W., Frieden, C., 1986. Actin polymerization: the mechanism of action of Cytochalasin D. J. Biol. Chem. 261, 15974–15980.

Harden, N., 2002. Signaling pathways directing the movement and fusion of epithelial sheets: lessons from dorsal closure in Drosophila. Differentiation 70, 181–203.

Hardin, J., Keller, R., 1988. The behaviour and function of bottle cells during gastrulation of *Xenopus laevis*. Development 103, 211–230.

Hertzler, P.L., Wang, S.W., Clark, W.H., 1994. Mesendoderm cell and archenteron formation in isolated blastomeres from the shrimp *Sicyonia ingentis*. Dev. Biol. 164, 333–344.

Holm, A., 1952. Experimentelle Untersuchugen uber die entwicklung und entwicklungphysiologie des spinnenembryos. Zool. Bidr. Upps. 25, 293–424.

Holtfreter, J., 1943. A study of the mechanics of gastrulation. Part I. J. Exp. Zool. 3, 261–318.

Jacinto, A., Baum, B., 2003. Actin in development. Mech. Dev. 120, 1337–1349.

Jacinto, A., Woolner, S., Martin, P., 2002. Dynamic analysis of dorsal closure in Drosophila: from genetics to cell biology. Dev. Cell 3, 9–19.

Jaffe, A.B., Hall, A., 2005. Rho GTPases: Biochemistry and Biology. Annu. Rev. Dev. Biol. 21, 247–269.

Kiehart, D.P., Galbraith, C.G., Edwards, K.A., Rickoll, W.L., Montague, R.A., 2000. Multiple forces contribute to cell sheet morphogenesis for dorsal closure in Drosophila. J. Cell. Biol. 149, 471–490.

Knaut, H., Pelegri, F., Bohmann, K., Schwarz, H., Nüsslein-Volhard, C., 2000. Zebrafish vasa RNA but not its protein is a component of the germ plasm and segregates asymmetrically before germline specification. J. Cell. Biol. 149, 875–888.

Kölsch, V., Seher, T., Fernandez-Ballester, G.J., Serrano, L., Leptin, M., 2007. Control of Drosophila gastrulation by apical localization of adherens junctions and RhoGEF2. Science 315, 384–386.

Lee, J.-Y., Goldstein, B., 2003. Mechanisms of cell positioning during *C. elegans* gastrulation. Development 130, 307–320.

Martin, A.C., Kaschube, M., Wieschaus, E.F., 2009. Pulsed contractions of an actin-myosin network drive apical constriction. Nature 457, 495–499.

Martin, A.C., Gelbart, M., Fernandez-Gonzalez, R., Kaschube, M., Wieschaus, E.F., 2010. Integration of contractile forces during tissue invagination. J. Cell. Biol. 188, 735–749.

Martin, P., Parkhurst, S.M., 2004. Parallels between tissue repair and embryo morphogenesis. Development 131, 3021–3034.

Mizuno, T., Amano, M., Kaibuchi, K., Nishida, Y., 1999. Identification and characterization of Drosophila homolog of Rho-kinase. Gene 238, 437–444.

Molyneaux, K., Wylie, C., 2004. Primordial germ cell migration. Int. J. Dev. Biol. 48, 537–544.

Nikolaidou, K.K., Barrett, K., 2004. A Rho GTPase signaling pathway is used reiteratively in epithelial folding and potentially selects the outcome of Rho activation. Curr. Biol. 14, 1822–1826.

Ozhan-Kizil, G., Havemann, J., Gerberding, M., 2009. Germ cells in the crustacean *Parhyale hawaiensis* depend on Vasa protein for their maintenance but not for their formation. Dev. Biol. 327, 230–239.

Price, A.L., Patel, N.H., 2008. Investigating divergent mechanisms of mesoderm development in arthropods: the expression of Ph-twist and Ph-mef2 in *Parhyale hawaiensis*. J. Exp. Zool. B Mol. Dev. Evol. 310, 24–40.

Price, A.L., Modrell, M.S., Hannibal, R.L., Patel, N.H., 2010. Mesoderm and ectoderm lineages in the crustacean *Parhyale hawaiensis* display intra-germ layer compensation. Dev. Biol. 341, 256–266.

Reed, B.H., Wilk, R., Schöck, F., Lipshitz, H.D., 2004. Integrin-dependent apposition of Drosophila extraembryonic membranes promotes morphogenesis and prevents anoikis. Curr. Biol. 14, 372–380.

Rehm, E.J., Hannibal, R.L., Chaw, R.C., Vargas-Vila, M.A., Patel, N.H., 2009a. Fixation and dissection of Parhyale hawaiensis embryos. ColdSpring Harb. Protoc., 127

pdb.prot5. Volume number: 1 of Emerging Model Organisms: A Laboratory Manual.
Rehm, E.J., Hannibal, R.L., Chaw, R.C., Vargas-Vila, M.A., Patel, N.H., 2009b. Antibody staining of Parhyale hawaiensis embryos. ColdSpring Harb. Protoc., 129 pdb.prot5. Volume number: 1 of Emerging Model Organisms: A Laboratory Manual.
Rehm, E.J., Hannibal, R.L., Chaw, R.C., Vargas-Vila, M.A., Patel, N.H., 2009c. Injection of Parhyale hawaiensis blastomeres with fluorescently labeledtracers. Cold Spring Harb. Protoc., 128. pdb.prot5. Volume number: 1 of Emerging Model Organisms: A Laboratory Manual.
Ridley, A.J., Schwartz, M.A., Burridge, K., Firtel, R.A., Ginsberg, M.H., Borisy, G., Parsons, J.T., Horwitz, A.R., 2003. Cell migration: integrating signals from front to back. Science 302, 1704–1709.
Riento, K., Ridley, A., 2003. Rocks: multifunctional kinases in cell behaviour. Nat. Rev. Mol. Cell Biol. 4, 446–456.
Roth, S., 2004. Gastrulation in other insects. In: Stern, C.D. (Ed.), Gastrulation: from cells to embryo, 1st ed. Cold Spring Harbor Laboratory Press, pp. 105–121.
Saaristo, M., 2006. Theridiid or cobweb spiders of the granitic Seychelles islands (Araneae, Theridiidae). Phelsuma 14, 49–89.
Sawyer, J.M., Harrell, J.R., Shemer, G., Sullivan-Brown, J., Roh-Johnson, M., Goldstein, B., 2010. Apical constriction: a cell shape change that can drive morphogenesis. Dev. Biol. 341, 5–19.
Scholtz, G., Wolff, C., 2002. Cleavage, gastrulation, and germ disc formation of the amphipod Orchestia cavimana (Crustacea, Malacostraca, Pericardia). Contrib. Zool. 71, 9–28.
Stern, C.D., 2004. Gastrulation: From Cells to Embryo, 1st ed. Cold Spring Harbor Laboratory Press, New York.
Winter, C., Wang, B., Ballew, A., Royou, A., Karess, R., Axelrod, J.D., Luo, L., 2001. Drosophila rho-associated kinase (Drok) links frizzled-mediated planar cell polarity signaling to the actin cytoskeleton. Cell 105, 81–91.
Wolff, C., Scholtz, G., 2002. Cell lineage, axis formation, and the origin of germ layers in the amphipod crustacean *Orchestia cavimana*. Dev. Biol. 250, 44–58.
Wray, G., Raff, R., 1991. Rapid evolution of gastrulation mechanisms in a sea urchin with lecithotrophic larvae. Evolution 45, 1741–1750.
Wu, S.-Y., Ferkowicz, M., McClay, D.R., 2007. Ingression of primary mesenchyme cells of the sea urchin embryo: a precisely timed epithelial mesenchymal transition. Birth Defects Res. C Embryo Today 81, 241–252.
Xu, N., Keung, B., Myat, M.M., 2008. Rho GTPase controls invagination and cohesive migration of the Drosophila salivary gland through crumbs and rho-kinase. Dev. Biol 321, 88–100.
Young, P.E., Richman, A.M., Ketchum, A.S., Kiehart, D.P., 1993. Morphogenesis in Drosophila requires nonmuscle myosin heavy chain function. Genes. Dev. 7, 29–41.